International Journal of Applied Engineering and Technology ISSN: 2277-212X (Online)
An Online International Journal Available at http://www.cibtech.org/jet.htm
2012 Vol. 2 (1) January-March, pp.23-29/Shanehsazzadeh and Sayedi
Research Article

OPTIMUM GEOMETRICAL PARAMETES FOR HALL SENSORS

***F. Shanehsazzadeh[1] and M. Sayedi[2]**
[1 2]Department of Electrical and Computer Engineering Electrical and Computer Engineering Dept.
Isfahan University of Technology
Isfahan, Iran - 84156-83111
**Author for Correspondence*

ABSTRACT
We looked for the best geometry that would maximize sensitivity of Hall sensors. Different shapes of Hall-effect sensors can transfer to rectangular one. So, our simulations are done on rectangular shape. Geometrical correction factor maximization was also performed for small sensing contacts Hall structures in order to ensure maximum sensitivity. The simulation is performed with Silvaco TCAD tool for special technology, Silterra standard CMOS technology. The present paper analyzes the influence of the dimensions, n-well and substrate doping concentration and distribution on the Hall-effect sensors performances.

Key Words: *Hall-effect sensor, Magnetic sensor, Geometrical Parameters, Active Region Concentration, Epitaxial Layer for Sensor*

INTRODUCTION
The potential application range of Hall-effect magnetic sensor is vast Ramsden (2006)**.** Such sensors are already widely utilized in the field of medicine, automotive and computer industry Popovic et al.(2001)- Pascal et al.(2008).
For those applications, the sensor should be generally integrated in a single chip. The sensing element (Hall device), the biasing electronics and also the signal processing are designed in the same chip Frick et al.(2007). Silicon Hall sensors are often the first candidates for such applications due to their cost-effective integration potential, reflecting in low cost, robustness and versatility Müller-Schwanneke et al.(2000).
The geometry plays a key role on the Hall-effect sensors performance and has been studied by the authors Paun et al.(2011).
The lack of accurate compact models of the Hall device leads the designer to utilize FEM-like complex or physical simulations to design the sensing element with an external tool in the integrated circuit design flow. The development of an efficient compact model of CMOS integrated Hall sensors is therefore a big factor that should improve design time and efficiency, and which could widen the applications range of Hall devices in integrated systems. So far, some compact models of Hall devices have been developed. The basic one is associated to resistors and current-driven voltage sources Jovanovic et al.(2004).
The present paper analyzes the influence of the dimensions, n-well and substrate doping concentration and distribution on the Hall-effect sensors performances, especially Hall voltage, with the aid of 3D physical simulations.

MATERIALS AND METHODS
In semiconductor materials, the classical carrier transport models Allegretto et al.(1991)–Selberherr(1984) is actually based on the continuity equations. For the complete description of semiconductor physical behavior, we also have to take into account the following partial differential equation of elliptic type
$div(\varepsilon grad V) = -q(p - n + N)$ (1)
Where V stands for the electrostatic potential, is the material electric permittivity, q represents the electron charge and n, p are particle densities for electrons and holes, respectively.

The electrostatic potential V solves the Poisson equation in (1) with $N = N_D - N_A$ denoting the fully ionized net impurity distribution.

We can mention that the magnetic induction effect reveals only in the definition relations of current density. In other words, the continuity equations and the Poisson's equation (1) stay the same as well in the magnetic field absence.

In fact, the distributions of electrostatic potential and current density in the device are fundamental to gain insight into the operating principles of the final artifact. This enables one to determine optimal parameters of an ideal semiconductor structure.

3D Hall cells simulations were performed by use of Silvaco TCAD tool, which solves the *Maxwell's equations*, both electrons and holes continuity equations. A three dimensional numerical modeling of carrier transport process in the magnetic field (electrostatic potential, current distributions) is used for semiconductor magnetic sensors with various geometries parameters.

The magnetic field which acts on the semiconductor structure for Hall voltage generation was handled by the galvanic transport model. Mobility was considered via doping dependence formula and recombination processes were taken into account by Shockley-Read-Hall and Auger model. In this regard, the ohmic contacts are considered ideal and the contact regions support a sufficiently high doping concentration. The carrier concentrations and electrostatic potential at the contact region are recommended by the usual boundary conditions of Dirichlet type.

The 3D Hall cell mesh includes a sufficient number of points for a good tradeoff between accuracy and simulation run time. Although Small meshing dimensions and a high number of points increase the accuracy of the results, it takes more CPU time and longer to execute. The mesh refinement window comprised a mesh step between 0.1 and 5µm on the three axes.

The meshed structure of one of the simulated Hall cell structures has been presented in Fig. 1.

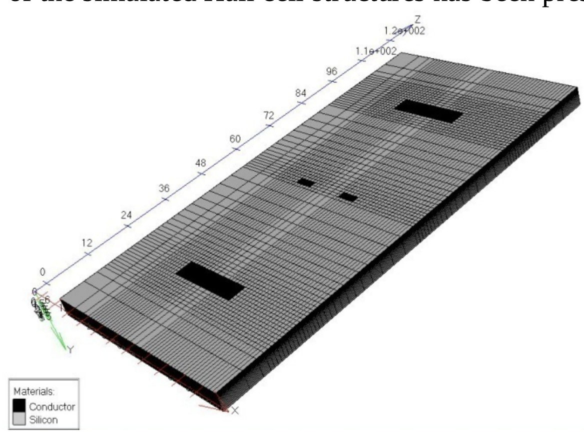

Figure 1: Hall plate sensor, which is simulated.

Different 3D Hall-effect sensor structures have been modeled. From the very beginning, all the cells were very accurately drawn, since any geometrical mismatch could significantly enhance the offset and affect some future current-spinning techniques implementations.

Classical rectangular sensor is simulated. The Hall cells were all modeled on a Silicon p-substrate with an n-well active region. Their size is $30 \times 90\ \mu m^2$. All the implemented structures basically follow the same fabrication process, by use of a p-substrate with concentration of 6+16 cm^{-3} and an active n-well region doped with concentration 6+18 cm^{-3}, in the form of a Gaussian profile implantation. The p-substrate and the n-doped layer are 5µm and 1µm thick respectively. These parameters are extracted from Silterra standard CMOS technology. In some parts of simulation, we need some changes in these parameters.

In general, V_{HALL} is defined by the following relation:

$$V_H = G_H \frac{R_H}{t} I B_{\perp}$$

The sensitivity of Hall sensor is also given by the relation:

$$S_I = G_H \frac{|R_H|}{t} = G_H \frac{1}{qnt}$$

Where B represents the magnetic field induction, G stands for the geometrical correction factor, I is the biasing current, n is the carrier density and t is the thickness of the active region Popovic(2004).

Since the V_H and consequently sensitivity are inversely proportional to the n-well doping concentration, a lightly doped n-well is normally used in the fabrication process. However, we simulate hall voltage for a range of n concentration and substrate concentration and distribution.

Each structure was equipped with four contacts, among which two are for biasing the device and the other two opposite ones for measurement purposes, by collecting the voltage drop for electrical tests purposes.

L and *W* are the cell length and width respectively, while *s* represents contact length. The width of the contacts is in general dictated by the technology used in the Hall cell fabrication process, and in our simulations, it was set at 2µm. The distance from the contacts to the n-well borders is 5µm.

For each simulated Hall cell structure, Hall voltage is simulated.

Table 1: The ranges of parameters change in simulations.

Dimension (w/l=3)(µm)	N-well doping concentration(cm^{-3})	Sub doping concentration(cm^{-3})	N-well doping distribution
25-50	1e17-1e19	1e14-5e17	Uniform - Gaussian

RESULTS AND DISCUSSION

Simulations were performed on all the structures using both voltage and current biasing without and with magnetic field. The biasing current was considered from 0 to 0.1 mA or the biasing voltage from 0 to 0.1 V. The current biasing was finally chosen for simulations, being closer to the real situation.

The results for sweeping n-well concentration, when other condition of sensors is constant, are presented in table 2. The results are viewed for 10µA. RRR

Table 2: Sweep n-well concentration between 1e17-1e19.

Concentration	1e17	4e17	1e18	4e18	6e18	1e19
Hall voltage(µv)	102.2	70	45.4	15.1	19.7	7

These results are presented in Fig. 2. Fit curve was evaluated by Matlab software,, which has been presented with solid line in Fig. 2. The relation between hall voltage and well concentration is presented in equation 2.

$$V_H = 1.04e\text{-}19\, n_{well}^{-1.3} \quad (2)$$

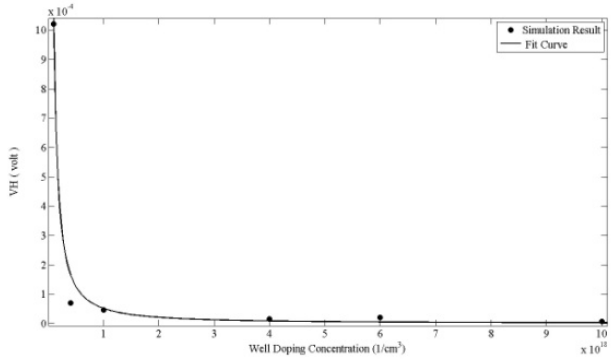

Figure 2: Hall voltage for different n-well concentration

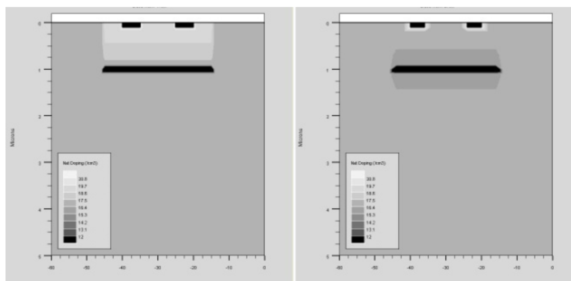

Figure 3: Different n-well distribution (1e19 left, 1e17 right)

As n-well concentration increases, hall voltage decreases resulting in, low doped concentration semiconductor for hall sensors.

For substrate concentration, the same work for n-well concentration was done.

Table 3: Sweep substrate concentration between 1e14-5e17

Concentration	1e14	5e14	1e15	5e15	1e16	6e16	1e17	5e17
Hall voltage(μv)	15.7	14.5	14	12.8	12.1	10.6	10.2	9.24

These values are presented in Fig. 4, too.

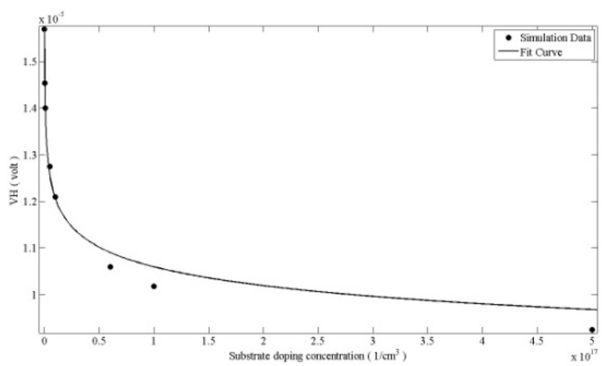

Figure 4: Hall voltage – substrate concentration curve

Fit curve has a relation like equation 3.

$V_H = 9.57e\text{-}5\ n_{sub}^{-0.06}$ (3)

If the substrate concentration is increased, as a result, Hall voltage increases. The influence of substrate concentration is different from n-well. N-well has a direct influence, whereas substrate changes distribution of well concentration.

However, it is optimized to choose minimum concentration for hall sensors, which is applied for substrate and active region of sensor. This is clear in Fig. 3-5.

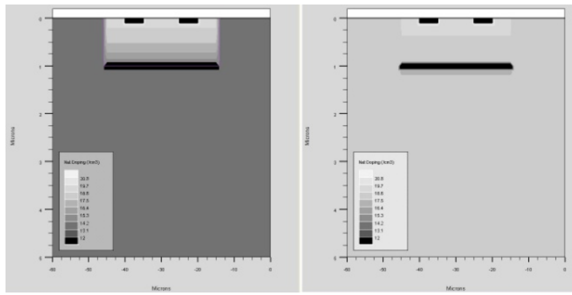

Figure 5: Different substrate concentration (1e14 (right), 5e17 (left)

With w/l constant with value 3, the value of width and length of rectangular are increased between 25-50.

Table 4: Sweep width and length for w/l=3

Width	25	30	40	50
Hall voltage(µv)	7.2	10.6	14.9	17.5

These values are shown in Fig. 6.

The equation is:

$V_H = (-1.08e\text{-}8)w^2 + (1.22e\text{-}6)w - (1.6e\text{-}5)$

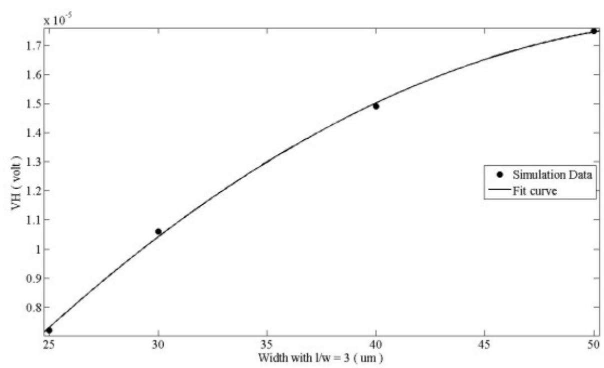

Figure 6: Hall voltage for different w and l while l/w is constant for Gaussian distribution

Hall voltage is increased by an increasing in dimensions of sensors, but this trend does not continue infinitely, as the dimensions are larger than the special value. This is traded off between hall voltage and space. Both critics are satisfied through choosing the correct dimensions.

The last simulation was done is simulating the same structure in uniform and Gaussian distribution, in n-well and epitaxial layer, respectively. We used p^+ region to restrict active region.

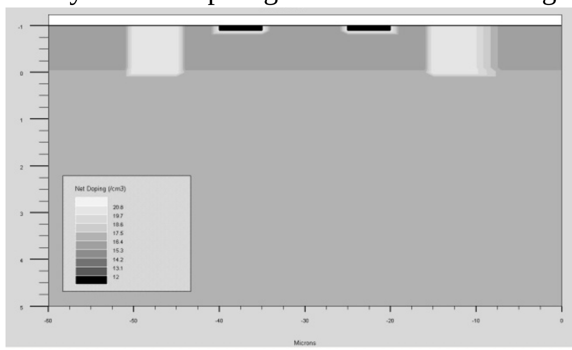

Figure 7: Rectangular hall plate sensor in epitaxial layer

The values for Gaussian and uniform distribution have been presented in table 4 and table 5 respectively.

Table 5: Sweep width and length of sensor in uniform layer

Width	25	30	40	50
Hall voltage(mv)	6.5	7.8	10.3	11.7

The relation is:

$$V_H = (-4.2e\text{-}6)w^2 + (5.3e\text{-}4)w - (4.05e\text{-}3)$$

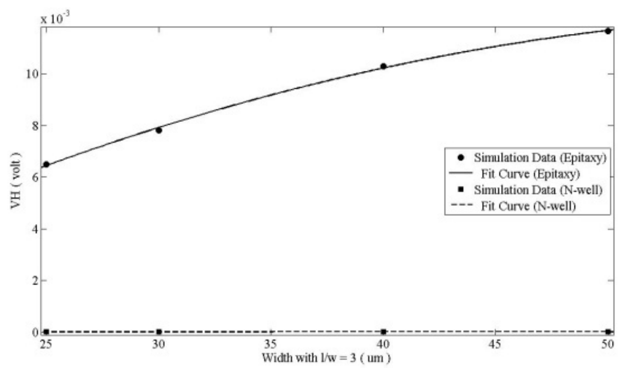

Figure 8: Hall voltage for different w and l while l/w is constant for uniform distribution

It is clear that hall voltage in the region with uniform distribution is much more than in a sample with Gaussian distribution. So, the sensors built in epitaxial layer are more sensitive.

From Fig. 9, it can be resulted in, here also there is a tradeoff, between space and dimensions, while l/w is kept constant. Because, after a special value the hall voltage is no longer increase with the speed as high as before it. So the designer should choose the right value for dimension to have an optimum sensor.

V_{HALL} estimations with 3D physical simulations using Silvaco TCAD tool were performed in order to analyze the influence of the dimensions, n-well and substrate doping concentration and distribution on the Hall-effect sensors performance.

The software allowed us to consider the magnetic field influence on semiconductors. Therefore, various Hall-effect sensors following a certain fabrication process were modeled. The parameters are extracted from Silterra standard CMOS technology.

These results, with the equations presented, can help to module hall sensors to be used in circuits with other circuit elements.

Now, we can choose best concentration and distribution for n-well and substrate and dimensions. Less concentration is better for hall sensors. Uniform distribution is best for hall sensors. At last, we have optimum value for hall sensor dimensions with constant ration between l and w. More other physical and structure parameters can be simulated for future work.

REFERENCES

AllegrettoW, Nathan A and Baltes H (1991). Numerical analysis of magnetic-field-sensitive bipolar devices. *IEEE Transactions on Computer-Aided Design of Integrated Circuits and Systems* **10**(4) 501 – 511.

Frick V, Pascal J, Hebrard L, Blonde JP and Felblinger J (2007). MOS integrated system for magnetic field monitoring and gradient measurement in MRI environment**.** in *50th Midwest Symposium on Circuits and Systems, MWSCAS, Montreal* 69 –72**.**

Jovanovic E, Pesic T and Pantic D (2004). 3D Simulation of Cross-Shaped Hall Sensors and its equivalent circuit model. in *24th International Conference on Microelectronics* 235-238.

Müller-Schwanneke C, Jost F, Marx K, Lindenkreuz S and von Klitzing K (2000). Offset reduction in silicon Hall sensors. *Sensors and Actuators A: Physical*. **81**(1-3) 18-22.

Ramsden E(2006). Hall-effect sensors: theory and applications. New York.

Selberherr IS(1984). Analysis and Simulation of Semiconductor Device. *Springer-Verlag*.

Pascal J, Hebrard L, Frick V and Blonde JP (2008). 3D Hall probe integrated in 0.35 µm CMOS technology for magnetic field pulses measurements. in *Joint 6th International IEEE Northeast Workshop on Circuits and Systems and TAISA Conference, NEWCAS-TAISA*. 97-100.

Paun MA, Sallese JM and Kayal M (2011). Geometrical parameters influence on the Hall effect sensors offset and drift. n *7th Conference on Ph.D. Research in Microelectronics and Electronics (PRIME), Trento*145-148.

Popovic RS, Randjelovic Z and Manic D (2001). Integrated Hall-effect. *Sensors and Actuators A: Physical* **91**(1-2) 46-50.

Popovic RS (2004). Hall Effect Devices, 2nd ed. *UK: Institute of Physics Publishing*.